Protein Science (1992), *1*, 236-244. Cambridge University Press. Printed in the USA.

Equilibrium denaturation studies of mouse β-nerve growth factor

DAVID E. TIMM[1] AND KENNETH E. NEET[1,2]

[1] Department of Biochemistry, Case Western Reserve University, Cleveland, Ohio 44106
[2] Department of Biological Chemistry, UHS/Chicago Medical School, North Chicago, Illinois 60064

(RECEIVED August 8, 1991; ACCEPTED September 23, 1991)

Abstract

Equilibrium denaturation of dimeric mouse β-nerve growth factor (β-NGF) has been studied by monitoring changes in the protein's spectroscopic characteristics. Denaturation of β-NGF in guanidine hydrochloride and urea resulted in an altered intrinsic fluorescence emission spectrum, fluorescence depolarization, and diminished negative circular dichroism. Native-like spectroscopic properties and specific biological activity are restored when denaturant is diluted from unfolded samples, demonstrating that this process is fully reversible. However, refolding of denatured β-NGF is dependent on the three disulfide bonds present in the native protein and does not readily occur when the disulfide bonds are reduced. Graphical analysis and nonlinear least-squares fitting of β-NGF denaturation data demonstrate that denaturation is dependent on the concentration of β-NGF and is consistent with a two-state model involving native dimer and denatured monomer ($N_2 = 2D$). The conformational stability of mouse β-NGF calculated according to this model is 19.3 ± 1.1 kcal/mol in 100 mM sodium phosphate at pH 7. Increasing the hydrogen ion concentration resulted in a 25% decrease in β-NGF stability at pH 4 relative to pH 7.

Keywords: β-nerve growth factor; denaturation; fluorescence; protein structure

Mouse β-nerve growth factor (β-NGF) is a basic protein composed of identical 118-residue subunits that associate through noncovalent interactions to form a 26-kDa homodimer (Greene & Shooter, 1980). β-NGF was predicted to contain 53–67% antiparallel β-sheet and 0–11% α-helix when analyzed by Raman spectroscopy (Williams et al., 1982), however; crystallographic analysis has been unavailable to date (Wlodawer et al., 1975). The primary sequence of β-NGF, including the positions of three intramolecular disulfide bonds, has been determined (Angeletti et al., 1973a,b). β-NGF is the initial member of a novel group of neurotrophic factors that includes the recently described brain-derived neurotrophic factor (Leibrock et al., 1989) and neurotrophin-3 (Hohn et al., 1990; Maisonpierre et al., 1990). Physiologically, β-NGF is secreted in a target-derived, paracrine manner (Levi-Montalcini & Calissano, 1979). Subsequent binding of β-NGF to specific receptors on sensory, sympathetic and central nervous system neurons results in a pleiotropic response that is essential for the development and survival of these cells.

Reprint requests to: Kenneth E. Neet, Department of Biological Chemistry, UHS/Chicago Medical School, 3333 Green Bay Rd., North Chicago, Illinois 60064.

Equilibrium denaturation studies, to date, have focused primarily on monomeric globular proteins. These studies provide a reasonable method for calculating the relatively small free energies involved in stabilizing the three-dimensional structure of a folded protein relative to random, unfolded forms (Pace, 1986). Additionally, solvent and thermal denaturation studies have been applied to the mutational analysis of recombinant proteins, including T4 lysozyme (Kitamura & Sturtevant, 1989) and RNase T1 (Shirley et al., 1989). These studies demonstrate that equilibrium denaturation can provide a sensitive measure of structural phenomena that may not be readily apparent, even in high-resolution crystallographic structures (Kitamura & Sturtevant, 1989; Weaver et al., 1989). Recently, equilibrium denaturation studies of the small dimeric globular proteins, f1 gene V protein (Liang & Terwilliger, 1991), P22 Arc repressor (Bowie & Sauer, 1989), and *Escherichia coli trp* aporepressor (Gittelman & Matthews, 1990), revealed that stable intermediates are not detected at equilibrium. The experimental data were consistent with a two-state model involving only the native dimer and denatured monomer. In contrast, the reversible dissociation and unfolding of *E. coli* aspartate aminotransferase was described by a four-state model in which two intermediate monomeric species could be de-

tected at defined denaturant concentrations (Herold & Kirschner, 1990).

Equilibrium denaturation studies of mouse β-NGF were undertaken with the purpose of defining structural characteristics necessary for studying β-NGF structure/function through mutational analysis. The results presented here suggest that, similar to gene V protein, P22 Arc, and the *trp* aporepressor, a two-state model describes the equilibrium between folded and unfolded β-NGF during denaturation.

Results

Guanidine hydrochloride (GdnHCl)-induced denaturation alters the spectroscopic properties of β-NGF

Unfolding of β-NGF results in decreased intrinsic fluorescence intensity and an increase (red shift) in the fluorescence emission maximum from 340 nm in the native state to 352 nm in the denatured state (Fig. 1A). Protein fluorescence following excitation at 295 nm is primarily due to the tryptophan side chain (Brand & Witholt, 1967; Lakowicz, 1983). The observed decrease in fluorescence intensity and the red-shifted emission maximum are consistent with the transfer of tryptophan residues from a hydrophobic environment in native β-NGF to aqueous solvent upon denaturation. β-NGF contains three tryptophan residues, two of which are accessible or partially accessible to solvent (Frazier et al., 1973; Cohen et al., 1980). Therefore, the altered fluorescence emission spectrum may be due to quenching of Trp 76 fluorescence by aqueous solvent in the denatured state.

Excitation of β-NGF at 280 nm results in an emission spectrum that undergoes similar changes in the presence of denaturant (Fig. 2). The relative fluorescence intensity (RFI) following excitation at 280 nm is approximately twice as great as that resulting from excitation at 295 nm (data not shown). The increased RFI may be due to more efficient excitation of tryptophan at 280 nm or to the excitation of tyrosine residues present in β-NGF.

Fluorescence depolarization also accompanies the denaturation of β-NGF. Native β-NGF has a steady-state fluorescence polarization value of 0.16 ± 0.01, whereas the denatured molecule has a value of 0.10 ± 0.01. A spherical molecule with a single exponential decay of polarization/anisotropy will have steady-state polarization/anisotropy described by the Perrin equation (Lakowicz, 1983). Steady-state polarization is dependent on temperature, viscosity, fluorescence lifetime, and the molecular volume. When measured under the conditions of low viscosity and dilute protein concentration, fluorescence depolarization is primarily due to increased rotational diffusion of the tryptophan fluorophore (Lakowicz, 1983). Dissociation of the β-NGF dimer into monomeric units is, therefore, expected to result in fluorescence depolarization. However, this interpretation is limited by the presence of three tryptophan residues that presumably contribute to the overall β-NGF steady-state fluorescence polarization. Furthermore, denaturation may lead to fluorescence depolarization by simply freeing fluorophore mobility about the C_α-C_β bond. Thus, the observed depolarization may be due to dissociation, unconstrained fluorophore rotation, or a combination of the two causes. Therefore, it is not clear whether the observed changes in fluorescence emission and fluorescence polarization provide measurements of separate or identical structural events (i.e., dissociation vs. unfolding).

Circular dichroism (CD) spectroscopy has also been used to monitor the GdnHCl-induced unfolding of β-NGF.

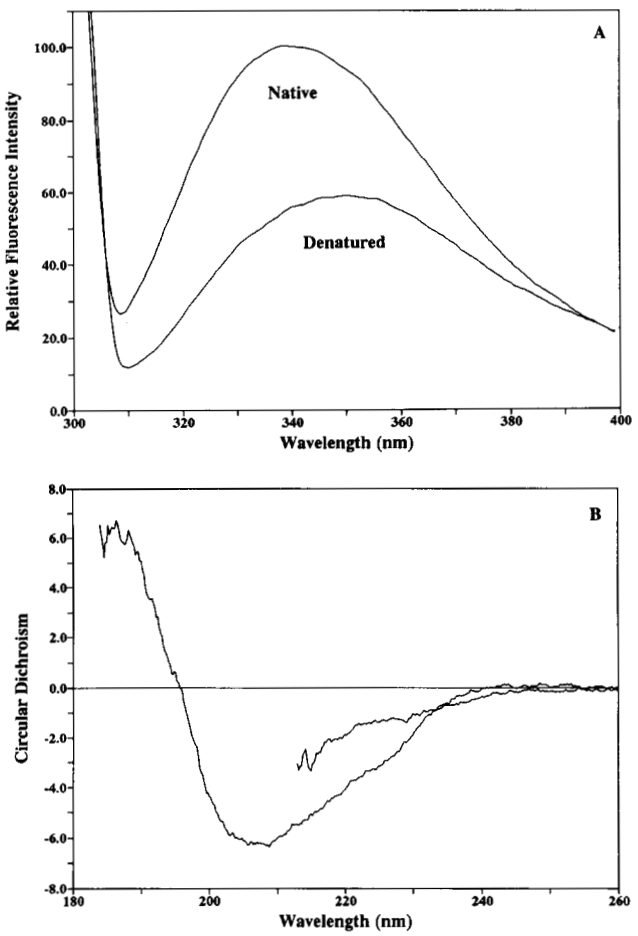

Fig. 1. Fluorescence emission and CD spectra of native and denatured β-NGF. **A:** The fluorescence emission spectra of native and denatured β-NGF were recorded from 300 to 400 nm following excitation at 295 nm. Samples contained 23 μg/mL β-NGF and 100 mM sodium phosphate pH 7. The denatured sample contains 4.8 M GdnHCl. **B:** The CD spectrum (° cm^2/dmol × 10^{-3}) of native β-NGF at 30 μg/mL in 10 mM sodium phosphate pH 6.8 was recorded from 184 to 260 nm in a 2-mm path length cuvette as an average of 12 scans. The CD spectrum of denatured β-NGF at 50 μg/mL containing 3.8 M GdnHCl and 100 mM sodium phosphate, pH 7, was recorded in a 4.5-mm path length cuvette from 260 to 210 nm as an average of six scans (as in Fig. 6).

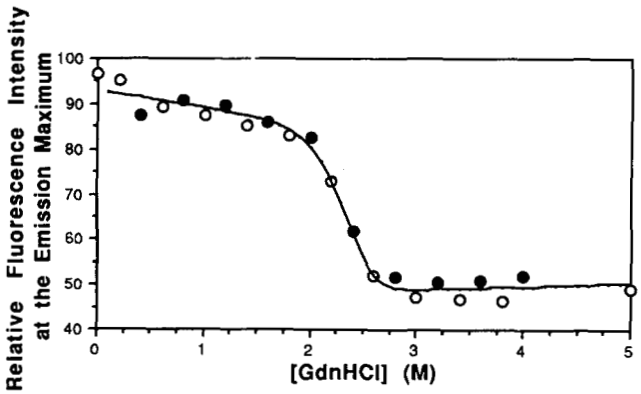

Fig. 2. GdnHCl equilibrium denaturation curve for β-NGF. The relative fluorescence intensity at the emission maximum following excitation at 280 nm is plotted versus the final GdnHCl concentration. RFI values of unfolded and refolded 30-μg/mL samples of β-NGF are represented as open and closed circles, respectively. The solid theoretical curve was fit to the data as described in Materials and methods with the native and denatured region slopes fixed at −3.8 and 0.75, respectively. The conformational stability calculated from nonlinear least-squares fitting of these data according to Equations 2 and 9 is 21.3 ± 2.5 kcal/mol and $m = -5.9 \pm 1.1$ kcal/mol/M.

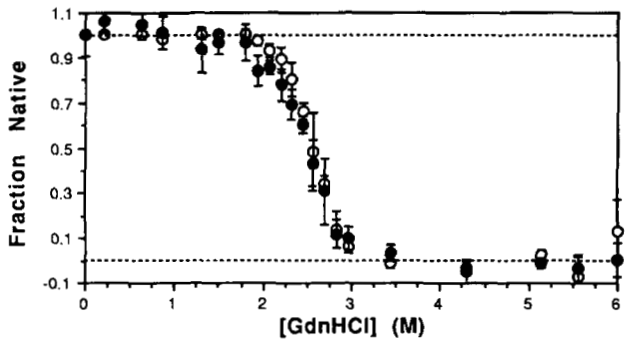

Fig. 3. The coincidence of denaturation curves monitored by fluorescence intensity and polarization. The fraction of native protein, calculated from relative fluorescence intensity at 320 nm (open circles) and fluorescence polarization values (closed circles, Equation 8) are plotted versus GdnHCl concentration. Individual points represent the mean ± SD for three separate experiments using 83 μg/mL β-NGF.

The CD observed below 230 nm is due to the peptide amide chromophore (Johnson, 1985) and can be used to estimate the content of secondary structure. The native β-NGF CD spectra (Fig. 1B) is characterized by a minimum near 208 nm, a maximum near 190 nm, and a negative to positive crossover at 196 nm. Upon denaturation the negative CD below 230 nm diminishes significantly (Fig. 1B), consistent with the loss of ordered secondary structure that should accompany protein unfolding. The CD spectra of denatured β-NGF are limited to these higher wavelengths by the denaturant absorption of light.

The shape and low amplitude of the CD spectra are consistent with a nonhelical protein, as predicted from Raman spectroscopy (Williams et al., 1982). The native CD spectrum in Figure 1B was used to estimate the secondary structural content of β-NGF by the variable selection method of Manavalan and Johnson (1987), which predicted 83% of the structure as 10 ± 5% α-helix, 23 ± 3% anti-parallel, and 6 ± 1% parallel β-sheet, 14 ± 2% turn, and 30 ± 2% other structures.

Denaturation of β-NGF is reversible and is consistent with a two-state model

A plot of relative fluorescence intensity (RFI) versus the denaturant concentration (Fig. 2) reveals a monophasic, sigmoidal curve, characteristic of a cooperative unfolding transition. The linear slope effects observed in both the native (below 2M GdnHCl) and denatured (above 3 M GdnHCl) regions of the curve are commonly observed in denaturant-induced unfolding curves (Pace, 1986) and are presumably due to solvent perturbation effects. Denaturation of β-NGF was found to be fully reversible when its three disulfide bonds remain intact. Native-like spectroscopic properties (Fig. 2) and specific biological activity (data not shown) were fully recovered when denatured samples were diluted to lower denaturant concentration (see Materials and methods). However, when denaturation was carried out in the presence of a reducing agent, the recovery of spectroscopic characteristics and biological activity upon dilution was low (less than 10%, data not shown). Denaturation curves constructed by following the shift in fluorescence emission maximum (data not shown) and fluorescence depolarization (Fig. 3) were coincident with those constructed from RFI data.

Several models could describe β-NGF denaturation at equilibrium depending on the contribution of different structural levels (secondary, tertiary, quaternary) to the overall stability of β-NGF. Two-state and multistate models have been applicable to the denaturation of small dimeric globular proteins at equilibrium (Bowie & Sauer, 1989; Gittelman & Matthews, 1990; Herold & Kirschner, 1990; Liang & Terwilliger, 1991). Noncoincident unfolding transitions measured by probes that are sensitive to different levels of protein structure and/or multiphasic transitions measured by the same probe are evidence for models with greater than two populated states. Consistent with a two-state model, the unfolding transition of β-NGF measured by fluorescence intensity and fluorescence depolarization are coincident and monophasic (Fig. 3). However, as previously stated, these probes may be sensitive to the same structural phenomenon.

With a dissociation constant below 10^{-12} M (Bothwell & Shooter, 1977), native β-NGF exists as a dimer at the concentrations used in this study. The two-state model for the denaturation of a dimeric protein, where only the native dimer and denatured monomer are significantly populated at equilibrium, is described by

$$N_2 = 2D, \quad (1)$$

where

$$K_D = [D]^2/[N_2] = 2Pt[f_d^2/(1 - f_d)]. \quad (2)$$

Pt is the total concentration of protein monomer. By the law of mass action, increasing the protein concentration will increase the proportion of native dimeric protein at every denaturant concentration, and the midpoint of the sigmoidal denaturation curve will increase as the protein concentration increases. Denaturation curves were constructed over a 15-fold range in β-NGF concentration (Fig. 4A) to determine if the unfolding of β-NGF at equilibrium is described by a two-state model. A protein concentration-dependent shift in the midpoint of the fluorescence unfolding transition was observed for β-NGF (Fig. 4A), consistent with this two-state model of denaturation.

The conformational stability ($\Delta G_D^{H_2O}$) of β-NGF was calculated according to the two-state model using graphical analysis and nonlinear least-squares fitting (see Materials and methods). Linear extrapolation of data from representative experiments at three β-NGF concentrations is shown in Figure 5, demonstrating the close agreement in $\Delta G_D^{H_2O}$ calculated according to the two-state model (Equations 2 and 9). Calculations were also made according to a three-state model assuming dissociation occurs at denaturant concentrations preceding the fluorescence transition and assuming fluorescence changes monitored the unfolding of a native-like monomer. The equilibrium constant for this model is

$$K_D = f_d/(1 - f_d). \quad (3)$$

As expected from the observed shift in transition midpoint, the $\Delta G_D^{H_2O}$ calculated according to this model was dependent on protein concentration (i.e., 5.8, 8.7, and 9.3 kcal/mol for 16.6, 83, and 250 μg/mL β-NGF, respectively) and are also lower than the free energy of the dimer dissociation alone. The two-state model, on the other hand, yielded values for the parameters, $\Delta G_D^{H_2O}$ and m, calculated graphically and by nonlinear least-squares fitting of denaturation data at different concentrations of β-NGF as summarized in Table 1. The values calculated over a 15-fold range in β-NGF concentration are in good agreement and, therefore, support the two-state model. These values are of similar magnitude to the values reported for the *E. coli trp* aporepressor (Gittelman & Matthews, 1990).

Urea-induced denaturation of β-NGF

Denaturation of β-NGF by urea resulted in the same spectroscopic changes described for GdnHCl. Denaturation resulted in decreased RFI, a red-shifted emission maximum, and fluorescence depolarization. Denaturation curves using urea were constructed as described for GdnHCl; however, the urea-induced change in β-NGF intrinsic fluorescence intensity followed a more complex pattern. A linear increase in RFI was observed below 2 M urea, followed by a plateau region preceding the unfolding transition (data not shown). The initial slope effect observed in RFI measurements was absent in fluorescence depolarization curves (Fig. 4B) and curves based on the shifted emission maximum (data not shown).

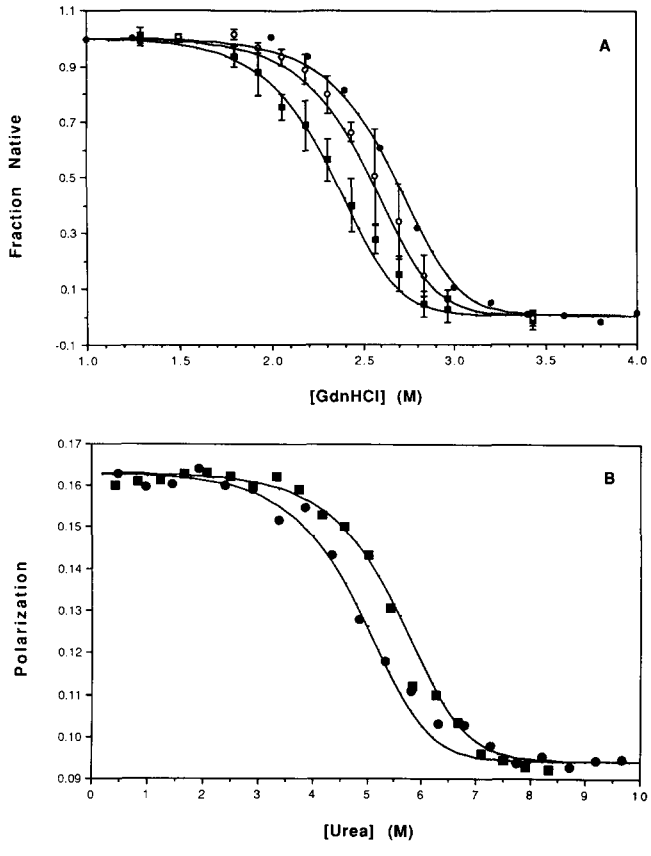

Fig. 4. The protein concentration dependence of β-NGF denaturation at two pH values. **A:** Relative fluorescence intensity at 320 nm following excitation at 295 nm was used to calculate the fraction of native protein at each denaturant concentration at pH 7 (100 mM sodium phosphate). Individual points represent the mean ± SD of four separate experiments at 16 μg/mL (filled squares), three experiments at 83 μg/mL (open circles), and a single experiment at 250 μg/mL (filled circles) β-NGF. Theoretical curves at each β-NGF concentration were generated according to Equations 2 and 9 with $\Delta G_D^{H_2O}$ and m set to 19.3 kcal/mol and 4.8 kcal/mol/M, respectively. **B:** The mean of triplicate fluorescence polarization determinations for single experiments at 20 (filled circles) and 100 (filled squares) μg/mL β-NGF concentration are plotted versus the urea concentration at pH 4 (100 mM sodium acetate). Theoretical curves were generated according to Equations 2 and 9 with $\Delta G_D^{H_2O}$ and m set to 14.7 kcal/mol and 1.4 kcal/mol/M, respectively.

Urea was less effective than GdnHCl for unfolding β-NGF. The unfolding transition in urea at neutral pH began at approximately 7 M and the midpoint of the unfolding curve, estimated from the fluorescence emission maximum and fluorescence depolarization (data not shown), occurred at approximately 9.5 M urea. Therefore, denaturation curves could not be analyzed in urea

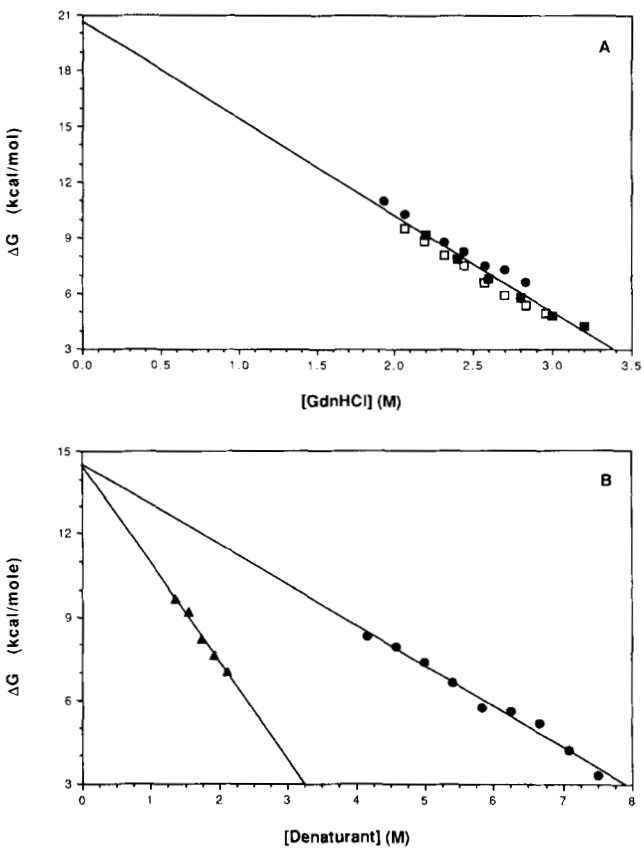

Fig. 5. ΔG_D as a function of denaturant concentration. **A:** The ΔG_D values for representative experiments at 16, 83, and 250 μg/mL β-NGF at pH 7 (circles, open squares, and closed squares, respectively) were calculated according to Equation 2 in the denaturation transition. The solid line was drawn by linear regression of the combined data and represents a calculated conformational stability of 20.6 kcal/mol and m = 5.3 kcal/mol/M according to Equation 9. **B:** The ΔG_D values for representative denaturation experiments at pH 4 were calculated in the transition region from fluorescence polarization measurements. Samples contained 20 μg/mL β-NGF in GdnHCl (triangles) and 100 μg/mL β-NGF in urea (circles). The extrapolations yield $\Delta G_D^{H_2O}$ values of 14.5 kcal/mol for β-NGF at pH 4.

at neutral pH. Complete denaturation was achieved in urea at acidic pH (Fig. 4B). Urea is commonly found to be two to three times less effective than GdnHCl as a denaturant. Approximately fourfold higher concentrations of urea were required to reach the midpoint of the fluorescence transition as compared to GdnHCl.

The conformational stability of β-NGF is decreased at acidic pH

When urea denaturation curves were constructed at acidic pH, a β-NGF concentration-dependent shift in the midpoint was also observed (Fig. 4B) and is consistent with the two-state equilibrium existing in GdnHCl. Denaturation curves in urea at pH 4 were, therefore, analyzed according to the two-state model. However, depolarization measurements were used as the basis for $\Delta G_D^{H_2O}$ calculations in urea, because the initial increase in RFI at low urea concentrations complicated defining the native region of the curve. Nonlinear least-squares analysis yielded $\Delta G_D^{H_2O}$ and m values of 14.7 ± 1.1 kcal/mol and 1.4 ± 0.2 kcal/mol/M (n = 2), respectively, at pH 4. Values within this range were also obtained by graphical analysis (Fig. 5B) and by fitting RFI data with points below 2 M urea omitted (data not shown). Low concentrations of urea may be inducing a conformational change in β-NGF, resulting in the initial increase in RFI. However, if this is the case, the conformational change has little effect on $\Delta G_D^{H_2O}$ compared to that calculated from GdnHCl curves at pH 4 (see below).

The effect of pH on β-NGF stability was further tested by constructing GdnHCl curves at pH 4. The increase in RFI that precedes denaturation in urea was not observed in GdnHCl curves at pH 4 (data not shown). This behavior is therefore due to the particular denaturant used and is not related to pH effects. Nonlinear least-squares analysis of GdnHCl denaturation curves at pH 4 based on

Table 1. *Gibb's free energies of unfolding for β-NGF calculated according to the two-state model*[a]

	Least-squares analysis		Graphical analysis		
[β-NGF] (μM monomer)	ΔG (kcal/mol)	m (kcal/mol/M)	ΔG (kcal/mol)	m (kcal/mol/M)	n
1.25	18.8 ± 0.6	4.4 ± 0.2	18.3 ± 1.2	4.2 ± 0.5	4
1.50	19.7 ± 0.9	5.2 ± 0.3	20.4 ± 1.6	5.5 ± 0.5	3
3.76[b]	17.9 ± 1.2	4.5 ± 0.5	17.2	4.2	1
6.24	19.7 ± 1.2	4.9 ± 0.5	19.9 ± 1.5	5.0 ± 0.6	3
18.8[b]	20.7 ± 0.8	5.3 ± 0.3	19.9	5.0	1
Mean	19.3 ± 1.0	4.8 ± 0.4	19.3 ± 1.6	4.8 ± 0.7	12

[a] Values were obtained by linear extrapolation analysis of GdnHCl denaturation curves buffered at pH 7 with 100 mM sodium phosphate. Values represent the mean ± SD for the indicated number of experiments.

[b] Standard deviations for experiments with n = 1 were derived from fitting and represent confidence levels for the converged values.

fluorescence depolarization yielded $\Delta G_D^{H_2O}$ and m values of 14.9 ± 0.5 kcal/mol and 3.7 ± 0.2 kcal/mol/M ($n = 2$), respectively. Results consistent with these values were also obtained by graphical analysis (Fig. 5B) and by fitting RFI curves (data not shown). The agreement in $\Delta G_D^{H_2O}$ values obtained in GdnHCl and urea at pH 4 indicates that a similar unfolded state is populated in both denaturants.

β-NGF is destabilized by 4–5 kcal/mol at pH 4 relative to pH 7. In the absence of denaturant, β-NGF remains at greater than 95% folded below pH 3 (data not shown). However, when the pH was varied in the presence of 4 or 6 M urea, denaturation occurred over 1–2 pH units with apparent pK values of approximately 3.5 and 5, respectively. With 10 acidic and 4 histidine residues present in β-NGF, the magnitude of the destabilization at acidic pH is expected to involve the titration of a limited number of these groups. The effect of salt on β-NGF (data not shown) was studied to determine if the protein could be destabilized through counterion shielding of electrostatic interactions. Denaturation of β-NGF by GdnHCl at pH 7 was not significantly affected by the presence of 1 M NaCl, and NaCl concentrations up to 3.8 M were unable to induce denaturation of β-NGF in 3 M urea at pH 4. Therefore, stabilizing electrostatic interactions may be inaccessible to Na^+, may not significantly contribute to $\Delta G_D^{H_2O}$, or are compensated by other possible salt effects such as hydrophobic interactions.

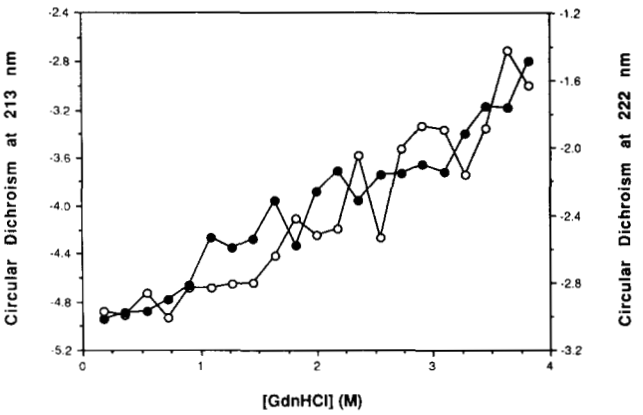

Fig. 6. Circular dichroism denaturation curve. The CD (° cm^2/dmol × 10^{-3}) of 50 μg/mL β-NGF in sodium phosphate pH 7 was measured as a function of GdnHCl concentration. Spectra were recorded in a 4.5-mm path length cuvette as an average of six scans. The CD at 213 nm (open circles) and 222 nm (solid circles) is plotted against the final GdnHCl concentration.

The unfolding of β-NGF monitored by CD

Denaturation curves generated by monitoring CD contrast with the cooperative sigmoidal curves based on the fluorescence properties of β-NGF. Curves generated by plotting CD against denaturant concentration show a broad change lacking a clear native or transition region (Fig. 6). Furthermore, these changes occur prior to and following the fluorescence-monitored transition. The anomalous behavior of CD-generated denaturation curves may be due to equilibrium conditions that vary from the two-state model used to interpret fluorescence measurements. The inconsistencies between the fluorescence and CD-monitored unfolding can be interpreted by a model in which multiple quasi-stable intermediates are formed under specific equilibrium conditions. Dimeric intermediates, characterized by nonnative secondary structures, become populated at GdnHCl concentrations preceding the fluorescence transition. Monomeric intermediates, containing residual secondary structure, might be populated at denaturant concentrations following the fluorescence transition but prior to complete unfolding. The calculated ΔG would then represent the unfolding of a tryptophan-containing core structure.

On the other hand, technical reasons may also account for the discrepancies between the different probes. Interpretation of the CD denaturation curve may be complicated by lack of a good reference position. The majority of proteins characterized by CD denaturation studies have substantial helical content, which affords a strong reference signal at 220 nm. β-NGF, in contrast, contains little helical secondary structure. Denaturation of RNase T1 and the gene V protein (Thomson et al., 1989; Liang & Terwilliger, 1991), which have high β-sheet content, has been monitored by CD at 238 nm and 229 nm, respectively. However, β-NGF lacks significant signals in these regions. Finally, the light-absorbing properties of denaturants prevent CD measurements at the β-NGF 208-nm negative minimum, which might provide a more meaningful reference wavelength.

Discussion

In light of this study and studies of other small dimeric proteins, it is apparent that dimeric protein structures are stabilized at different levels. The contribution of intrachain and interchain interactions to the overall protein conformational stability can vary significantly. A three-state model of the equilibrium dissociation and unfolding of a dimeric protein, simplified to involve only native dimer (N_2), folded monomer (N), and unfolded monomer (D), describes possible variations in the intrachain and interchain contributions to $\Delta G_D^{H_2O}$:

$$N_2 = 2N = 2D, \tag{4}$$

where

$$K_1 = [N]^2/[N_2] \quad \text{and} \quad K_2 = [D]/[N]. \tag{5}$$

For proteins with K_1 significantly larger than K_2, the quaternary interactions stabilizing dimeric association will be less than the secondary and tertiary interactions stabilizing the folded monomer. Conditions will, therefore, exist in which an intermediate (i.e., folded monomer) is populated to a greater extent than the native dimer or denatured monomer. The monomeric intermediate structure may not be identical to the structure of subunits in the native dimer; however, some native-like structure presumably persists. The opposite extreme involves a situation in which K_2 is much larger than K_1. Quaternary interactions contribute the vast majority of the overall $\Delta G_D^{H_2O}$, and the equilibrium constants for dissociation and denaturation will be indistinguishable. Dissociation, therefore, leads to the formation of an intrinsically unstable species and a folded monomeric species will not be significantly populated at equilibrium.

The P22 Arc repressor and *E. coli* aspartate aminotransferase serve as examples of the extreme situations described above. The $\Delta G_D^{H_2O}$ calculated for P22 Arc from equilibrium denaturation is essentially equal to the free energy associated with its dissociation constant alone (Bowie & Sauer, 1989). Folded monomer, therefore, is not expected to be significantly populated at equilibrium. A two-state model involving folded dimer and unfolded monomer describes this protein at equilibrium because the folded monomer is not stabilized relative to the unfolded form. According to this model, folded Arc is primarily stabilized through quaternary interactions. In contrast, the unfolding and dissociation of aspartate aminotransferase (Herold & Kirschner, 1990) at equilibrium results in the formation of two folded monomeric species that are stabilized relative to unfolded monomer. Based on spectral properties, the structures of the monomeric intermediates are not identical to that found in the dimer. However, intrachain interactions are sufficient to stabilize the folded structure in the absence of interchain interactions. This situation implies that secondary and tertiary interactions contribute greater stabilization to the overall stability than quaternary interactions.

Analysis of β-NGF denaturation by RFI and fluorescence polarization measurements reveals a coincident, monophasic transition with a midpoint that increases with increasing protein concentration. These results are consistent with a two-state transition involving folded dimer and unfolded monomer. The results of CD measurements complicate this model, and the equilibrium may actually involve a more complex situation involving a transition between nonnative dimeric and monomeric intermediates. However, the aforementioned uncertainties associated with our CD measurements cause us to favor the two-state model. $\Delta G_D^{H_2O}$ calculations based on this model in GdnHCl are internally consistent over a 15-fold range of protein concentration at neutral pH and in urea and GdnHCl at an acidic pH. Furthermore, similar transitions are observed when tryptophan fluorescence is measured following excitation at 295 nm or at 280 nm (Figs. 2, 4A). Changes in tryptophan fluorescence following excitation at 295 nm may represent localized structural perturbations. However, the fluorescence transition following excitation at 280 nm presumably includes contributions from two tyrosine residues and may represent a more global structural change.

The β-NGF $\Delta G_D^{H_2O}$ value of 19.3 kcal/mol calculated according to the two-state model is slightly lower than that reported for the *trp* aporepressor (Gittelman & Matthews, 1990). The reported dissociation constant of less than 10^{-12} M at pH 7 (Bothwell & Shooter, 1977) has an associated free energy of greater than 16.3 kcal/mol. Therefore, β-NGF provides an example intermediate to the extremes of Arc and Asp aminotransferase. At β-NGF concentrations above 10^{-12} M and in the absence of denaturant, folded dimer would be the predominant species. Folded monomer would be stabilized relative to unfolded monomer by less than 3 kcal/mol, a value less than that observed for many monomeric globular proteins (Pace, 1990). Therefore, in contrast to Arc, a significant equilibrium could exist between folded dimers and both folded and unfolded monomers at less than picomolar concentration. Under the conditions used in denaturation experiments, however, the two-state model presumably applies because the amount of denaturant necessary to detect denaturation destabilizes the monomer sufficiently enough to prevent detection of the folded monomer. This situation contrasts with that observed for Asp aminotransferase, in which quaternary interactions can be destabilized under conditions in which secondary and tertiary interactions retain stability.

In addition to providing a measure of the overall conformational stability ($\Delta G_D^{H_2O}$), the model describing the equilibrium denaturation of a protein can provide insight into the relative contribution of different levels of interaction to protein structure. Our findings are consistent with a model in which greater than 70% of the overall conformational stability of β-NGF at pH 7 is contributed by noncovalent interchain/quaternary interactions. At pH 4 a similar situation holds with overall stability decreasing by 4.4 kcal/mol (Fig. 5) and dimer stability decreasing by as much as 3 kcal/mol (Moore & Shooter, 1975). We propose that this stabilization accounts for the occurrence of β-NGF as a dimer, independent of requirements for biological function. Furthermore, evolutionary divergence of amino acids that might destabilize the monomer could be allowed in a protein thermodynamically stabilized as a dimer.

Materials and methods

Protein and reagents

β-NGF was purified as previously described (Smith et al., 1968; Stach et al., 1977; Woodruff & Neet, 1986) and stored at −20 °C in 0.4% acetic acid, 0.15 M NaCl, pH

4.0. Protein concentrations were determined using $A^{1\%} = 16.0$ at 280 nm. Concentrated GdnHCl and urea stock solutions were prepared fresh using distilled, deionized water and ultrapure-grade reagents from Boehringer Mannheim, ICN, and U.S. Biochemicals.

Equilibrium denaturation experiments

Equilibrium denaturation was performed by incubating individual samples of β-NGF at each denaturant concentration buffered with 0.1 M sodium phosphate or 0.1 M sodium acetate at room temperature (23 ± 2 °C). The reversibility of denaturation was demonstrated by initially denaturing samples in 4 M GdnHCl, pH 7, for 2–24 h followed by dilution to the final denaturant concentration. Equilibrium was achieved rapidly in 4 M GdnHCl as judged by manual mixing experiments in which full spectral changes were complete in less than 1 min. However, equilibration of samples within the transition region of unfolding experiments required 48 h, and refolding experiments required up to 72 h for the full recovery of spectroscopic characteristics. The specific biological activity of refolded samples was determined as the concentration required to elicit half maximal neurite outgrowth in a defined media bioassay using PC12 cells (Greene, 1977). The reversibility of samples denatured in urea and GdnHCl at pH 4 was demonstrated by treatments similar to those described above.

Fluorescence measurements

Fluorescence measurements were made using a Perkin-Elmer LS-5B spectrofluorometer, and emission spectra were recorded on a Perkin-Elmer GP-100 Graphics Printer. Samples were commonly excited at 295 nm, with the exception of a single experiment at 280 nm. Samples were measured in a Helma quartz microcuvette (25 mm^2 cross section) with volumes of 250–300 μL. Protein concentrations used in these experiments (16–250 μg/mL) were determined to be in the linear range of instrument response; thus, inner filter effects were neglected.

Steady-state fluorescence polarization was measured by single channel instrumentation using a manual polarizer accessory installed in the emission and excitation paths. Polarization was calculated as

$$P = [(I_{II})_V - G(I_I)_V]/[(I_{II})_V + G(I_I)_V], \quad (6)$$

where

$$G = (I_{II})_H/(I_I)_H. \quad (7)$$

The emission intensity is measured parallel $(I_{II})_V$ and perpendicular $(I_I)_V$ to the vertically polarized plane of excitation light, and the correction factor (G) is calculated by measuring the parallel and perpendicular emission intensities following excitation with horizontally polarized light. This correction factor had a value of 1.4 and accounts for the different efficiencies that the excitation and emission monochromators have for horizontally and vertically polarized light (Lakowicz, 1983). Polarization measurements were made with excitation and emission wavelengths of 295 and 340 nm, respectively. The change in relative fluorescence intensity that occurs upon denaturation was accounted for using the following equation (Lakowicz, 1983) to calculate the fraction of denatured protein (f_d) from polarization data:

$$f_d = [(P - P_n)/(P_d - P)R + (P - P_n)]. \quad (8)$$

R is the ratio of the denatured to native fluorescence intensities at each denaturant concentration, P is the observed polarization, and P_n and P_d are the native and denatured polarization values, respectively.

CD measurements

CD spectra were recorded using a Jasco J600 spectropolarimeter, and data were processed using software provided by Jasco and a Wyse (IBM compatible) computer. Measurements were made on β-NGF samples of 30–100 μg/mL in quartz cuvettes of 2 or 4.5 mm path length. Spectra were typically recorded as an average of 6–12 scans from 260 nm to 184 nm, depending on denaturant concentration.

Graphical analysis of denaturation curves

Conformational stability calculations were based on the relative fluorescence intensity (RFI) at 320 nm (except where noted), because differences between the folded and unfolded β-NGF spectra were relatively larger at this wavelength. Experimental deviations for RFI measurements were also smaller than polarization measurements. Determinations based on fluorescence polarization or RFI at other than 320 nm yielded values consistent with those calculated at 320 nm.

Linear extrapolation analysis of denaturation data was performed as described (Pace, 1986). RFI was plotted as a function of denaturant concentration. The linear portions of the plots, preceding and following the denaturation transition and representing values observed for the folded (Yn) and unfolded (Yd) protein, were defined by linear regression. These values were extrapolated into the nonlinear portion of the graph. The fraction of unfolded protein (f_d) at each denaturant concentration was calculated as the ratio of the difference between the measured value (Y) and the folded value to the difference between the folded and unfolded values ($f_d = Y - Yn/Yd - Yn$). Equilibrium constants (K_D) and the corresponding Gibb's free energies of unfolding ($\Delta G_D = -RT \ln[K_D]$) were then calculated at each denaturant concentration in the transition region (see Results). The linear dependence of ΔG_D on denaturant concentration observed in the transition was assumed to continue to zero denaturant concentration (Schellman, 1978). Extrapolation to zero

denaturant concentration was used to calculate the conformational stability of the protein in the absence of denaturant ($\Delta G_D^{H_2O}$) by the following relationship:

$$\Delta G_D = \Delta G_D^{H_2O} - m\,[\text{denaturant}]. \quad (9)$$

Analysis of denaturation curves by nonlinear least-squares fitting

In order to minimize bias in defining the folded, unfolded, and transition regions of denaturation curves, $\Delta G_D^{H_2O}$ was calculated from raw denaturation data with the program BASICFIT written in BASIC for the Macintosh computer that uses a Marquardt gradient-analytical search (Bevington, 1969) with six variable parameters. The slopes and Y-intercepts of the linear native and denatured regions of the curve, and the equilibrium constant, K_D, and the dependence of the Gibb's free energy of unfolding, m, on the denaturant concentration (Equation 9), defining the transition region, were iteratively fit to RFI or polarization values. Due to complications in fitting six variable parameters, convergence was often restricted to initial parameter estimates in the range of ±50% of the final fitted value. However, within this range, initial estimates did not significantly affect converged values.

Acknowledgments

We thank Drs. P.L. de Haseth and J.E. Jentoft for valuable discussion during manuscript preparation. This paper is from the Protein Structure/Function Group at CWRU. This work was supported by a National Institutes of Health, USPHS, grant NS24380 and by a National Science Foundation Instrumentation grant, DIR88-20739. D.E.T. was supported by a National Institutes of Health training grant GM08056.

References

Angeletti, R.H., Hermodson, M.A., & Bradshaw, R.A. (1973a). Amino acid sequences of mouse 2.5S nerve growth factor. II. Isolation and characterization of the thermolytic and peptic peptides and the complete covalent structure. *Biochemistry 12*, 100–115.

Angeletti, R.H., Mercanti, D., & Bradshaw, R.A. (1973b). Amino acid sequences of mouse 2.5S nerve growth factor. I. Isolation and characterization of the soluble tryptic and chymotryptic peptides. *Biochemistry 12*, 90–100.

Bevington, P.R. (1969). *Data Reduction and Error Analysis for the Physical Sciences.* McGraw-Hill, New York, New York, pp. 235–237.

Bothwell, M.A. & Shooter, E.M. (1977). Dissociation equilibrium constant of β-nerve growth factor. *J. Biol. Chem. 23*, 8532–8536.

Bowie, J.U. & Sauer, R.T. (1989). Equilibrium dissociation and unfolding of the Arc repressor dimer. *Biochemistry 28*, 7139–7143.

Brand, L. & Witholt, B. (1967). Fluorescence measurements. *Methods Enzymol. 11*, 776–856.

Cohen, P., Sutter, A., Landreth, G., Zimmerman, A., & Shooter, E.M. (1980). Oxidation of tryptophan-21 alters the biological activity and receptor binding characteristics of mouse nerve growth factor. *J. Biol. Chem. 255*, 2949–2954.

Frazier, W.A., Hogue-Angeletti, R.A., Sherman, R., & Bradshaw, R.A. (1973). Topography of mouse 2.5S nerve growth factor. Reactivity of tyrosine and tryptophan. *Biochemistry 12*, 3281–3293.

Gittelman, M.S. & Matthews, C.R. (1990). Folding and stability of *trp* aporepressor from *Escherichia coli*. *Biochemistry 29*, 7011–7020.

Greene, L.A. (1977). A quantitative assay for nerve growth factor (NGF) activity employing a clonal pheochromocytoma cell line. *Brain Res. 133*, 350–353.

Greene, L.A. & Shooter, E.M. (1980). The nerve growth factor: Biochemistry, synthesis, and mechanism of action. *Annu. Rev. Neurosci. 3*, 353–402.

Herold, M. & Kirschner, K. (1990). Reversible dissociation and unfolding of aspartate aminotransferase from *Escherichia coli*: Characterization of a monomeric intermediate. *Biochemistry 29*, 1907–1913.

Hogue-Angeletti, R. (1970). The role of the tryptophan residues in the activity of the nerve growth factor. *Biochim. Biophys. Acta 214*, 478–482.

Hohn, A., Leibrock, J., Bailey, K., & Barde, Y.A. (1990). Identification and characterization of a novel member of the nerve growth factor/brain-derived neurotrophic factor family. *Nature 344*, 339–341.

Kitamura, S. & Sturtevant, J.M. (1989). A scanning calorimetric study of the thermal denaturation of the lysozyme of phage T4 and the Arg 96 to His mutant form thereof. *Biochemistry 28*, 3788–3792.

Johnson, W.C. (1985). Circular dichroism and its empirical application to biopolymers. *Methods Biochem. Anal. 31*, 61–163.

Lakowicz, J.R. (1983). *Principles of Fluorescence Spectroscopy.* Plenum Press, New York, New York.

Leibrock, J., Lottspeich, F., Hohn, A., Hofer, M., Hengerer, B., Masiakowski, P., Thoenen, H., & Barde, Y.A. (1989). Molecular cloning and expression of brain-derived neurotrophic factors. *Nature 341*, 149–152.

Levi-Montalcini, R. & Calissano, P. (1979). The nerve growth factor. *Sci. Am. 240*, 66–77.

Liang, H. & Terwilliger, T.C. (1991). Reversible denaturation of the gene V protein of bacteriophage f1. *Biochemistry 30*, 2772–2782.

Maisonpierre, P.C., Belluscio, L., Squinto, S., Ip, N.Y., Furth, M.E., Lindsay, R.M., & Yancopoulos, G.D. (1990). Neurotrophin-3: A neurotrophic factor related to NGF and BDNF. *Science 247*, 1446–1451.

Manavalan, P. & Johnson, W.C. (1987). Variable selection method improves the prediction of protein secondary structure from circular dichroism spectra. *Anal. Biochem. 167*, 76–85.

Moore, J.B. & Shooter, E.M. (1975). The use of hybrid molecules in a study of the equilibrium between nerve growth factor monomers and dimers. *Neurobiology 5*, 369–381.

Pace, C.N. (1986). Determination and analysis of urea and guanidine hydrochloride denaturation curves. *Methods Enzymol. 131*, 266–282.

Pace, C.N. (1990). Conformational stability of globular proteins. *Trends Biochem. Sci. 15*, 14–17.

Schellman, J.A. (1978). Solvent denaturation. *Biopolymers 17*, 1305–1322.

Shirley, B.A., Stanssens, P., Steyaert, J., & Pace, C.N. (1989). Conformational stability and activity of ribonuclease T1 and mutants. *J. Biol. Chem. 264*, 11621–11625.

Smith, A.P., Greene, L.A., Fisk, H.R., Varon, S., & Shooter, E.M. (1968). Multiple forms of nerve growth factor protein and its subunits. *Biochemistry 7*, 3259–3268.

Stach, R.W., Wagner, B.J., & Stach, B.M. (1977). A more rapid method for the isolation of the 7S nerve growth factor complex. *Anal. Biochem. 83*, 26–32.

Thomson, J.A., Shirley, B.A., Grimsley, G.R., & Pace, C.N. (1989). Conformational stability and mechanism of folding of ribonuclease T1. *J. Biol. Chem. 264*, 11614–11620.

Weaver, L.H., Gray, T.M., Gruetter, M.G., Anderson, D.E., Wozniak, J.A., Dahlquist, F.W., & Matthews, B.W. (1989). High resolution structure of the temperature-sensitive mutant of phage lysozyme, Arg 96 to His. *Biochemistry 28*, 3793–3797.

Williams, R., Gaber, B., & Gunning, J. (1982). Raman spectroscopic determination of the secondary structure of crystalline nerve growth factor. *J. Biol. Chem. 257*, 13321–13323.

Wlodawer, A., Hodgson, K.O., & Shooter, E.M. (1975). Crystallization of nerve growth factor from mouse submaxillary glands. *Proc. Natl. Acad. Sci. USA 72*, 777–779.

Woodruff, N.R. & Neet, K.E. (1986). β-nerve growth factor binding to PC12 cells. Association kinetics and cooperative interactions. *Biochemistry 25*, 7956–7966.